Transactions of the Nigerian Association of Mathematical Physics
Volume 7, (March, 2018), pp135 – 142

NUMERICAL ANALYSIS OF ABRASIVE WEAR IN HOT FORGING DIES

C.I. Oviawe[1], O. Oviawe[2] and L.Ucho[3]

Department of Mechanical Engineering, Edo State Polytechnic, Usen, P.M.B. 1104, Benin City, Edo State.
[2]Deparmtent of Mathematics, College of Education, Ekiadolor, Benin, P.M.B 1114, Benin City.
[3]Department of Physics, College of Education, Ekiadolor, P.M.B. 1154, Benin City.

Abstract

This paper presents a mathematical model for predicting abrasive wear in hot forging dies. T he main objective of the study is to solve the developed model using the Galerkin's Finite Element Method. The governing differential equation of the developed mathematical model was put in a weaker form in order to obtain the stiffness matrix, mass matrix and source vector that is generated for each element to get the depth of wear at nodal points. The wear stiffness matrix, mass matrix and source vector were assembled by enforcing continuity for the nodal degree of freedom to obtain the global system equations. A time approximation was developed using α -family of interpolation and to achieve this, we apply the Crank-Nicholson finite difference scheme taking (α -0.5) and a time step $\Delta t = 0.005$ was used to compute the depth of wear. From the validation of this work model with experimental data and exact results we had a correlation coefficient of 0.9999, it can be concluded that the model have strong tendency for higher degree of accuracy and efficiency.

Keywords: Forging, Dies, Galerkin's Crank-Nicholson, α -family.

1.0 Introduction

In hot forging , the abrasive particles are the main cause of die wear which is developed by mechanical friction between die surface and workpiece. These particles can damage the die surface progressively during each die stroke. The abrasive particles may be hard oxides or scales, external contaminating particles or other hard carbides dislodged from the die surface. Abrasive wear results in removal of die material from the surface and its amount depends on numerous parameters such as temperature, surface roughness, sliding distance, relative velocity, material, contact force and lubrication. Due to its complicated nature, it is difficult to formulate relationship between parameters and amount of die wear. Several works have been reported in the literature. Painter et al.[1] analyzed the die wear in the hot extrusion using the finite element code DEFORM to simulate the process and wear program to predict the wear condition Huber et al [2] presented a very efficient, incremental implementation of Archard's wear model on the global scale for pin wear and disc wear in a pin-on-disc tribometer. Zamani and Bigalari [3] examined the wear profile on die surface during the hot forging operation for an axisymmetric cross-section. Lejla et al. [4] work on analysis of the main types of damage on industrial upper and lower hot forging dies for hot forging of car steering mechanisms.

Other studies [5] concentrated on the life of industrial dies and molds. They have focused on how the life of die can be efficaciously increased by timely repair of damaged surfaces. Rachopol and Sasithom [6] carried out a study of wear and life enhancement of hot forging dies using finite element analysis. In this paper, we present wear analysis of hot forging dies using the Galerkin finite element method.

2.0 Mathematical Modeling

$$\frac{d^2h}{dv^2} + \frac{dh}{dv} - km = \frac{m}{F}\frac{dh}{dt} \quad 0 \le v \le h \qquad (2.1)$$

Equation (2.1) is the developed model differential governing equation Oviawe [7].
The associated boundary conditions are given by:

Corresponding Author: Oviawe C.I., Email: iyekowa@yahoo.co.uk, Tel: +2348055805619

$h(o,t)=0$ and $\frac{dh}{dt}(v_f,t)=0$ (2.2)

Initial condition $h(V,o)=h_o$ (2.3)

In modeling equation (2.1), the following assumptions were made:

a) The die was assumed to be homogenous and possessed isotropic hardness oHRC54 initially before forging
b) The surface of the die possessed no surface treatment
c) No heat loss from the work-piece during the transport from furnace to die
d) Abrasive wear was assumed to be the dominated wear mechanism
e) Uniform billet temperature with average grain size (20 μm) before setting on the die
f) Initial temperature of workpiece (1100°C)
g) Initial temperature of die (300°C)

2.1 Material and Methods

The spatial domain of the wear divided into a number of uniform linear element. Stiffness matrix, mass matrix, source vector and flux vector were generated for each element using Galerkin finite element method to get the wear depth at nodal points. The stiffness matrix, mass matrix, source vector and flux vector were assembled by enforcing continuity of the nodal degree of freedom to obtain the global system equations. The linear interpolation shape functions were used to obtain a solution

A time approximation was developed using the α -family of interpolation in which a weighted average of the time derived of the dependent variable (h) is approximated at two consecutive time steps by linear interpolation of the values of the variable at two steps. We then apply the Grank-Nicholson finite difference scheme by taking α =0.5 and a time step $(\Delta t = 0.005)$ to obtain equation for the solution. A numerical analysis was done to compare the finite element results with the exact solution.

2.2 Weak Formulation

The weak form of equation (2.1) is obtained by multiplying the equation by a weight function $W = w(t)$ and integrating it over the domain of the element and since it is time dependent and this becomes

$$\int_o^h w(t)\frac{d^2h}{dv^2}dv + \int_o^h w(t)\frac{dh}{dv}dv - \int_o^h w(t)kmdv - \int_o^h w(t)\frac{m}{F}\frac{dh}{dt}dv = 0 \quad (2.4)$$

The term $\frac{d^2h}{dv^2}$ was put in the weakerform by reducing to the order $\frac{dh}{dv}$ using integrating by arts principles

$$\int_o^h w(t)\left\{\frac{d}{dv}\left(\frac{dh}{dv}\right)\right\}dv = \left[w(t)\frac{dh}{dv}\right]_o^h - \int_o^h \frac{dw}{dv}\cdot\frac{dh}{dv}dv \quad (2.5)$$

Substituting the weak form equation (2.5) into equation (2.4)

$$\int_o^h \frac{dh}{dv}\cdot\frac{dw}{dv}dv + \int_o^h w(t)\frac{dh}{dv}dv - \int_o^h w(t)kmdv - \int_o^h w(t)\frac{M}{F}\frac{dh}{dt}dv - \left[w(t)\frac{dh}{dv}\right]_o^h = 0 \quad (2.6)$$

2.3 Finite Element Modeling (FEM)

Let the solution of equation (2.6) be of the separable variable form

$$h(v,t) \approx h^e(v,t) = \sum_{j=1}^{n} h_j^e(t)\psi_j^e(v) \quad (2.7)$$

In Finite element form equation (2.7) becomes

$$h(v,t) = \sum_{j=1}^{n} h_j^e(t)\psi_j^e(v) = \sum_{j=1}^{n} h_j^e(t)\psi_j^e(v) \quad (2.8)$$

Where ψ_j^e is the shape interpolation function at jth nodes and h_j^e the depth of wear at jth node of the element. Since Galerkin finite element is to be adopted in the research, we assumed that the weight function is equal to interpolation function.

That is:

$$w(t) = \psi_j^e(v) \quad (2.9)$$

Substituting equation (2.9) into equation (2.6) we obtain:

$$\int_o^h \frac{d}{dv}\sum h_j^e(t)\psi_j^e(v)\frac{d\psi_j^e}{dv}(v)dv + \int_o^h \psi_j^e(v)\frac{d}{dv}\sum h_j^e(t)\psi_j^e(v) - \int_o^h \psi_j^e(v)kmdv$$

$$-\frac{m}{F}\int_o^h \psi_j^e(v)\frac{d}{dv}\sum h_j^e(t)\psi_j^e(v) - \left[\psi_j^e(v)\frac{d}{dv}\sum h_j^e\right]_o^h = 0 \qquad (2.10)$$

Equation (2.8) can be translated in matrix form as:

$$\left[K_{uj}^2\right]\{h\} + \left[M_{ij}^e\right]\{h\} = \{F_j^e\} + \{Q_j^e\} \qquad (2.11)$$

Where

$\left[K_{ij}^e\right]$ = wear coefficient matrix

$\left[M_{ij}^e\right]$ = wear mass matrix

$\{F_j^e\}$= source vector

$\{Q_j^e\}$ = flux vector

Equation (2.11) is the finite element model (FEM) for the analysis

$$\left[K_{ij}^e\right] = \left(\int_o^h \frac{d}{dv}\psi_i^e(v)\frac{d}{dv}\psi_j^e(v) + \int_o^h \psi_i^e(v)\frac{d\psi_j^e}{dv}(v)\right)dv \qquad (2.12)$$

$$\left[M_{ij}^e\right] = \frac{m}{F}\int_o^h \left(\psi_j^e(v)\right)dv \qquad (2.13)$$

$$\{F_j^e\} = km\int_o^h \left(\psi_i^e(v)\right)dv \qquad (2.14)$$

$$\{Q_j^e\} = \int_o^h \left(\psi_i^e(v)\frac{d\psi_j^e}{dv}(v)\right)dv \qquad (2.15)$$

Using the shape functions for linear interpolation [8],

$$\psi_1^e = \left(1 - \frac{v}{h_e}\right) \qquad (2.16)$$

$$\psi_2^e = \left(\frac{v}{h_e}\right) \qquad (2.17)$$

2.4 Calculations of wear coefficient matrix $\left[K^e\right]$

$$k_{11}^e = \left\{\left(\int_o^h \frac{d}{dv}\psi_1^e\frac{d}{dv}\psi_1^e\right) + \left(\int_o^h \psi_1^e\frac{d}{dv}\psi_1^e\right)\right\}dv \qquad (2.18)$$

$$k_{11}^e = \left(\frac{1}{h_e} - \frac{1}{2}\right) \qquad (2.19)$$

$$k_{12}^e = \left\{\left(\int_o^h \frac{d}{dv}\psi_1^e\frac{d}{dv}\psi_2^e\right) + \left(\int_o^h \psi_1^e\frac{d}{dv}\psi_2^e\right)\right\}dv \qquad (2.20)$$

$$k_{12}^e = \left(\frac{-1}{h_e} + \frac{1}{2}\right) \qquad (2.21)$$

$$k_{21}^e = \left\{\left(\int_o^h \frac{d\psi_2^e}{dv}\frac{d\psi_1^e}{dv}\right) + \left(\int_o^h \psi_2^e\frac{d\psi_1^e}{dv}\right)\right\}dv \qquad (2.22)$$

$$k_{21}^e = \left(\frac{-1}{h_e} - \frac{1}{2}\right) \qquad (2.23)$$

$$k_{22}^e = \left\{\left(\int_o^h \frac{d\psi_2^e}{dv}\frac{d\psi_2^e}{dv}\right) + \left(\int_o^h \psi_2^e\frac{d\psi_2^e}{dv}\right)\right\}dv \qquad (2.24)$$

$$k_{22}^e = \left(\frac{1}{h_e} + \frac{1}{2}\right) \qquad (2.25)$$

$$k_{ij}^e = \begin{bmatrix} k_{11}^e & k_{12}^e \\ k_{21}^e & k_{22}^e \end{bmatrix} \qquad (2.26)$$

Substituting equations (2.19, 2.21, 2.23 and 2.25) into equation (2.26) to obtained the general form of wear coefficient matrix

$$k^e = \frac{1}{2h}\begin{bmatrix} 2-h & -2+h \\ -2-h & 2+h \end{bmatrix} \tag{2.27}$$

2.5 Calculations of wear mass matrix $\left[M^e\right]$

$$M_{11}^e = \frac{m}{F}\int_o^h \left(\psi_1^e \psi_1^e\right) dv \tag{2.8}$$

$$M_{11}^e \left(\frac{Mh}{3F}\right) \tag{2.9}$$

$$M_{12}^e = \frac{M}{F}\int_o^h \left(\psi_1^e \psi_2^e\right) dv \tag{2.30}$$

$$M_{12}^e = \left(\frac{Mh}{6F}\right) \tag{2.31}$$

$$M_{21}^e = \frac{M}{F}\int_o^h \left(\psi_1^e \psi_2^e\right) dv \tag{2.32}$$

$$M_{21}^e = \left(\frac{mh}{6F}\right) \tag{2.33}$$

$$M_{22}^e = \frac{M}{F}\int_o^h \left(\psi_2^e \psi_2^e\right) dv \tag{2.34}$$

$$M_{22}^e = \left(\frac{Mh}{3F}\right) \tag{2.35}$$

$$\left[M_{ij}^e\right] = \begin{bmatrix} M_{11}^e & M_{12}^e \\ M_{12}^e & M_{22}^e \end{bmatrix} \tag{2.36}$$

Substituting equations (2.29, 2.31, 2.33 and 2.35) into equation (2.36) to obtain the general form of wear mass matrix.

$$\left[M^e\right] = \frac{mh}{6F}\begin{bmatrix} 2 & 1 \\ 1 & 2 \end{bmatrix} \tag{2.37}$$

2.6 Calculations of source vector $\left\{F^e\right\}$

$$F_1^e = km\int_o^h \left(\psi_1^e\right) dv \tag{2.38}$$

$$F_1^e = \left(\frac{Kmh}{2}\right) \tag{2.39}$$

$$F_2^e = km\int_o^h \left(\psi_2^e\right) dv \tag{2.40}$$

$$F_2^e = \left(\frac{Kmh}{2}\right) \tag{2.41}$$

$$F_j^e = \begin{Bmatrix} F_1^e \\ F_2^e \end{Bmatrix} \tag{2.42}$$

$$F^e = \frac{kmh}{2}\begin{Bmatrix} 1 \\ 1 \end{Bmatrix} \tag{2.43}$$

2.7 Assembly of Global Equations

We assembled the elements equations to obtain the equations for the whole wear matrix.

$$\left[K^e\right] = \begin{bmatrix} K_{11}^1 & K_{12}^1 & 0 & 0 & 0 & 0 & 0 & 0 & 0 \\ K_{21}^1 & K_{22}^1 + K_{11}^2 & K_{12}^2 & 0 & 0 & 0 & 0 & 0 & 0 \\ 0 & 0 & K_{22}^2 + K_{11}^3 & K_{12}^e & 0 & 0 & 0 & 0 & 0 \\ 0 & 0 & K_{21}^2 & K_{22}^3 + K_{11}^4 & K_{12}^4 & 0 & 0 & 0 & 0 \\ 0 & 0 & 0 & M_{21}^4 & K_{22}^4 + K_{11}^5 & K_{12}^5 & 0 & 0 & 0 \\ 0 & 0 & 0 & 0 & K_{21}^5 & K_{22}^5 + K_{11}^6 & K_{12}^6 & 0 & 0 \\ 0 & 0 & 0 & 0 & 0 & K_{21}^6 & K_{22}^6 + K_{11}^7 & K_{12}^7 & 0 \\ 0 & 0 & 0 & 0 & 0 & 0 & K_{21}^7 & K_{22}^7 + K_{11}^8 & K_{12}^8 \\ 0 & 0 & 0 & 0 & 0 & 0 & 0 & K_{21}^8 & K_{22}^8 \end{bmatrix} \tag{2.44}$$

$$[M^e]=\begin{bmatrix} M_{11}^1 & M_{12}^1 & 0 & 0 & 0 & 0 & 0 & 0 & 0 \\ M_{21}^1 & M_{22}^1+M_{11}^2 & M_{12}^2 & 0 & 0 & 0 & 0 & 0 & 0 \\ 0 & 0 & M_{22}^2+M_{11}^3 & M_{12}^e & 0 & 0 & 0 & 0 & 0 \\ 0 & 0 & M_{21}^2 & M_{22}^3+M_{11}^4 & M_{12}^4 & 0 & 0 & 0 & 0 \\ 0 & 0 & 0 & M_{21}^4 & M_{22}^4+M_{11}^5 & M_{12}^5 & 0 & 0 & 0 \\ 0 & 0 & 0 & 0 & M_{21}^5 & M_{22}^5+M_{11}^6 & M_{12}^6 & 0 & 0 \\ 0 & 0 & 0 & 0 & 0 & M_{21}^6 & M_{22}^6+M_{11}^7 & M_{12}^7 & 0 \\ 0 & 0 & 0 & 0 & 0 & 0 & M_{21}^7 & M_{22}^7+M_{11}^8 & M_{12}^8 \\ 0 & 0 & 0 & 0 & 0 & 0 & 0 & M_{21}^8 & M_{22}^8 \end{bmatrix} \quad (2.45)$$

$$\{F^e\}=\begin{Bmatrix} F_1^1 \\ F_2^1+F_1^e \\ F_2^3+F_1^3 \\ F_2^3+F_1^4 \\ F_2^4+F_1^5 \\ F_2^5+F_1^6 \\ F_2^6+F_1^7 \\ F_2^9 \end{Bmatrix} \quad (2.46$$

2.8 Assembled Wear Matrices

$$[K^e]=\frac{1}{2h}\begin{bmatrix} 2-h & -2+h & 0 & 0 & 0 & 0 & 0 & 0 & 0 \\ -2-h & 4 & -2+h & 0 & 0 & 0 & 0 & 0 & 0 \\ 0 & -2-h & 4 & -2+h & 0 & 0 & 0 & 0 & 0 \\ 0 & 0 & -2-h & 4 & -2+h & 0 & 0 & 0 & 0 \\ 0 & 0 & 0 & -2-h & 4 & -2+h & 0 & 0 & 0 \\ 0 & 0 & 0 & 0 & -2-h & 4 & -2+h & 0 & 0 \\ 0 & 0 & 0 & 0 & 0 & -2-h & 4 & -2+h & 0 \\ 0 & 0 & 0 & 0 & 0 & 0 & -2-h & 4 & -2+h \\ 0 & 0 & 0 & 0 & 0 & 0 & 0 & -2-h & 2+h \end{bmatrix} \quad (2.47)$$

$$[M^e]=\frac{Mh}{6F}\begin{bmatrix} 2 & 1 & 0 & 0 & 0 & 0 & 0 & 0 & 0 \\ 1 & 4 & 1 & 0 & 0 & 0 & 0 & 0 & 0 \\ 0 & 1 & 4 & 1 & 0 & 0 & 0 & 0 & 0 \\ 0 & 0 & 1 & 4 & 1 & 0 & 0 & 0 & 0 \\ 0 & 0 & 0 & 1 & 4 & 1 & 0 & 0 & 0 \\ 0 & 0 & 0 & 0 & 1 & 4 & 1 & 0 & 0 \\ 0 & 0 & 0 & 0 & 0 & 1 & 4 & 1 & 0 \\ 0 & 0 & 0 & 0 & 0 & 0 & 1 & 4 & 1 \\ 0 & 0 & 0 & 0 & 0 & 0 & 0 & 1 & 2 \end{bmatrix} \quad (2.48)$$

$$\{F^e+Q^e\}=\frac{Kmh}{2}\begin{Bmatrix} 1 \\ 2 \\ 2 \\ 2 \\ 2 \\ 2 \\ 2 \\ 2 \\ 1 \end{Bmatrix}+\begin{Bmatrix} Q_1^1 \\ Q_2^1+Q_1^2 \\ Q_2^2+Q_1^3 \\ Q_2^3+Q_1^4 \\ Q_2^4+Q_1^5 \\ Q_2^5+Q_1^6 \\ Q_2^7+Q_1^8 \\ Q_2^9 \end{Bmatrix} \quad (2.50)$$

2.9 Final Assembly

This is achieved by substituting equations (2.48, 2.49 and 2.50) into equation (2.11) to obtain:

$$\frac{1}{2h}\begin{bmatrix} 2-h & -2+h & 0 & 0 & 0 & 0 & 0 & 0 & 0 \\ -2-h & 4 & -2+h & 0 & 0 & 0 & 0 & 0 & 0 \\ 0 & -2-h & 4 & -2+h & 0 & 0 & 0 & 0 & 0 \\ 0 & 0 & -2-h & 4 & -2+h & 0 & 0 & 0 & 0 \\ 0 & 0 & 0 & -2-h & 4 & -2+h & 0 & 0 & 0 \\ 0 & 0 & 0 & 0 & -2-h & 4 & -2+h & 0 & 0 \\ 0 & 0 & 0 & 0 & 0 & -2-h & 4 & -2+h & 0 \\ 0 & 0 & 0 & 0 & 0 & 0 & -2-h & 4 & -2+h \\ 0 & 0 & 0 & 0 & 0 & 0 & 0 & -2-h & 2+h \end{bmatrix}\begin{Bmatrix} h_1 \\ h_2 \\ h_3 \\ h_4 \\ h_5 \\ h_6 \\ h_7 \\ h_8 \\ h_9 \end{Bmatrix}+$$

$$=\frac{Mh}{6F}\begin{bmatrix}2&1&0&0&0&0&0&0&0\\1&4&1&0&0&0&0&0&0\\0&1&4&1&0&0&0&0&0\\0&0&1&4&1&0&0&0&0\\0&0&0&1&4&1&0&0&0\\0&0&0&0&1&4&1&0&0\\0&0&0&0&0&1&4&1&0\\0&0&0&0&0&0&1&4&1\\0&0&0&0&0&0&0&1&2\end{bmatrix}\begin{Bmatrix}\dot{h}_1\\\dot{h}_2\\\dot{h}_3\\\dot{h}_4\\\dot{h}_5\\\dot{h}_6\\\dot{h}_7\\\dot{h}_8\\\dot{h}_9\end{Bmatrix}=\frac{Kmh}{2}\begin{Bmatrix}1\\2\\2\\2\\2\\2\\2\\2\\1\end{Bmatrix}+\begin{Bmatrix}Q_1^1\\Q_2^1+Q_1^2\\Q_2^2+Q_1^3\\Q_2^3+Q_1^4\\Q_2^4+Q_1^5\\Q_2^5+Q_1^6\\Q_2^6+Q_1^7\\Q_2^7+Q_1^8\\Q_2^9\end{Bmatrix}$$

Due to balance of internal fluxes, it follows that:

$$Q_2^1+Q_1^2=Q_2^3+Q_1^4=Q_2^5+Q_1^6=Q_2^7+Q_1^8=0 \tag{2.52}$$

$$Q_2^2+Q_2^4=Q_2^6=0 \tag{2.53}$$

Substituting equations (2.52 and 2.53) into equation (2.51) gives

$$\frac{1}{2h}\begin{bmatrix}2-h&-2+h&0&0&0&0&0&0&0\\-2-h&4&-2+h&0&0&0&0&0&0\\0&-2-h&4&-2+h&0&0&0&0&0\\0&0&-2-h&4&-2+h&0&0&0&0\\0&0&0&-2-h&4&-2+h&0&0&0\\0&0&0&0&-2-h&4&-2+h&0&0\\0&0&0&0&0&-2-h&4&-2+h&0\\0&0&0&0&0&0&-2-h&4&-2+h\\0&0&0&0&0&0&0&-2-h&2+h\end{bmatrix}\begin{Bmatrix}h_1\\h_2\\h_3\\h_4\\h_5\\h_6\\h_7\\h_8\\h_9\end{Bmatrix}+$$

$$=\frac{Mh}{6F}\begin{bmatrix}2&1&0&0&0&0&0&0&0\\1&4&1&0&0&0&0&0&0\\0&1&4&1&0&0&0&0&0\\0&0&1&4&1&0&0&0&0\\0&0&0&1&4&1&0&0&0\\0&0&0&0&1&4&1&0&0\\0&0&0&0&0&1&4&1&0\\0&0&0&0&0&0&1&4&1\\0&0&0&0&0&0&0&1&2\end{bmatrix}\begin{Bmatrix}\dot{h}_1\\\dot{h}_2\\\dot{h}_3\\\dot{h}_4\\\dot{h}_5\\\dot{h}_6\\\dot{h}_7\\\dot{h}_8\\\dot{h}_9\end{Bmatrix}=\frac{Kmh}{2}\begin{Bmatrix}1\\2\\2\\2\\2\\2\\2\\2\\1\end{Bmatrix}+\begin{Bmatrix}Q_1^1\\0\\0\\0\\0\\0\\0\\0\\Q_2^9\end{Bmatrix} \tag{2.54}$$

We considered the boundary conditions

$h(o,t)=0$ and $\frac{dh}{dt}(v_f,t)=0$

Initial condition : $h(v,o)=h_o$ which implies that

$$\frac{1}{2h}\begin{bmatrix}4&-2+h&0&0&0&0&0\\-2&4&-2+4&0&0&0&0\\0&-2-h&4&-2+h&0&0&0\\0&0&-2-h&4&-2+h&0&0\\0&0&0&-2-h&4&-2+h&0\\0&0&0&0&-2-h&4&-2+h\\0&0&0&0&0&0&4\end{bmatrix}\begin{Bmatrix}h_2\\h_3\\h_4\\h_5\\h_6\\h_7\\h_8\end{Bmatrix}+$$

$$\frac{Mh}{6F}\begin{bmatrix}4&1&0&0&0&0&0\\1&4&-2+4&0&0&0&0\\0&1&4&1&0&0&0\\0&0&-2-h&4&1&0&0\\0&0&0&1&4&1&0\\0&0&0&0&1&4&1\\0&0&0&0&0&1&4\end{bmatrix}\begin{Bmatrix}\dot{h}_2\\\dot{h}_3\\\dot{h}_4\\\dot{h}_5\\\dot{h}_6\\\dot{h}_7\\\dot{h}_8\end{Bmatrix}=\frac{Kmh}{2}\begin{Bmatrix}2\\2\\2\\2\\2\\2\\2\end{Bmatrix} \tag{2.55}$$

3.0 Time Approximation

In this study, we developed a time approximation using α-family of interpolation and to achieve this, we apply the crank-Nicholson finite difference scheme and taken (α=0.5) and time step $\Delta t=0.005$ was used to compute the depth of wear as shown in equation (2.56).

$$\{h\}_{s+1} = \left[[M^e] + \frac{\Delta t}{2}[k^e]\right]^{-1}\left[[M^e] - \frac{\Delta t}{2}[k^e]\right]\{h\}_s + \frac{\Delta t}{2}\{Q^e\} \qquad (2.56)$$

4.0 Results and Discussion

Finite element method is used to simulate the hot forging operation. The Matlab software programming is used to obtain wear depth of the die. The parameters affecting the wear like contact time, sliding velocities and contact force were obtained from numerical results of the forging simulation. Tale 1 shown the comparison between wear depth of finite element and exact results. It is observed that the results the simulation approximates fast to the exact results as the numbers of element are increased. Fig 1 is the plot of wear depth against contact time. At $t = 0$, beginning of the hot forging die operation, workpiece and die are in initial contact and depth of wear is zero. It is observed that at $t = 1.50$ seconds the die reaches to its maximum depth of wear due to the friction between workpiece and die. But, as the forging operation progresses, the wear rate becomes uniform throughout, the process. Fig.2 shows the relationship between sliding velocity and depth of wear. It is observed that as the forging progresses the sliding velocity increases linearly with wear depth. But, at 75 percent of the operation time (3.75 seconds), the maximum wear depth in the die was 1.5181mm and at this time of operation, the maximum sliding velocity for the exact solution is 1.483m/s while that of finite element simulation is 1.379m/s which is approximately the same as that of exact solution. While Fig.3 shows the plot of wear depth against contact force and it is observed that as the force increases the wear depth increases and produced a parabolic profile and the highest depth of wear values of contact force appears at 80 percent of operation time on the die with a value of 300KN

Table 1: Comparison between wear depth of Finite Element analysis and Exact results for (α=0.5, and Δt =0.005)

Elements / Time (s)	2LE wear depth (mm)	3LE wear depth (mm)	4LE wear depth (mm)	5LE wear depth (mm)	6LE wear depth (mm)	7LE wear depth (mm)	8LE wear depth (mm)	EXACT wear depth (mm)
0.0000	1.0000	1.0000	1.0000	1.0000	1.0000	1.0000	1.0000	1.0000
0.0500	1.0836	1.0503	1.0516	1.0536	1.0538	1.0537	1.0536	1.0536
0.1000	1.1451	1.1160	1.1074	1.1067	1.1070	1.1071	1.1072	1.1072
0.1500	1.1911	1.1769	1.1664	1.1629	1.1617	1.1613	1.1611	1.1606
0.2000	1.2261	1.2278	1.2206	1.2168	1.2151	1.2142	1.2137	1.2124
0.2500	1.2533	1.2687	1.2665	1.2642	1.2629	1.2621	1.2616	1.2603
0.3000	1.2749	1.3012	1.3040	1.3039	1.3036	1.3033	1.3031	1.3024
0.3500	1.2925	1.3269	1.3343	1.3363	1.3371	1.3375	1.3377	1.3384
0.4000	1.3071	1.3475	1.3585	1.3625	1.3644	1.3655	1.3661	1.3682
0.4500	1.3196	1.3641	1.3779	1.3836	1.3865	1.3881	1.3892	1.3926
0.5000	1.3304	1.3776	1.3936	1.4006	1.4043	1.4064	1.4078	1.4125
0.5500	1.3400	1.3889	1.4064	1.4144	1.4187	1.4212	1.4229	1.4285
0.6000	1.3486	1.3983	1.4169	1.4256	1.4304	1.4332	1.4351	1.4415
0.6500	1.3565	1.4064	1.4257	1.4349	1.4399	1.4431	1.4451	1.4521
0.7000	1.3637	1.4134	1.4330	1.4425	1.4479	1.4511	1.4533	1.4607
0.7500	1.3704	1.4196	1.4393	1.4490	1.4545	1.4578	1.4601	1.4677
0.8000	1.3766	1.4250	1.4448	1.4545	1.4600	1.4635	1.4657	1.4736
0.8500	1.3825	1.4300	1.4495	1.4593	1.4648	1.4682	1.4705	1.4784
0.9000	1.3880	1.4345	1.4537	1.4634	1.4689	1.4723	1.4746	1.4825
0.9500	1.3931	1.4386	1.4575	1.4670	1.4724	1.4758	1.4781	1.4859
1.0000	1.3980	1.4424	1.4609	1.4702	1.4756	1.4789	1.4811	1.4889
1.0500	1.4027	1.4459	1.4640	1.4731	1.4784	1.4816	1.4838	1.4914
1.1000	1.4071	1.4492	1.4668	1.4757	1.4809	1.4841	1.4862	1.4936
1.1500	1.4112	1.4522	1.4694	1.4781	1.4831	1.4863	1.4883	1.4956

Variation of Wear depth with time for (Linear Elements)

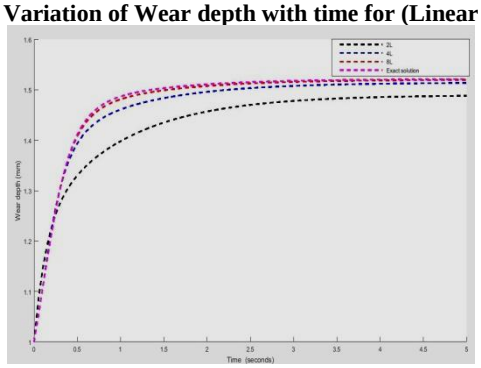

Fig .1: A graph of wear depth against change in time

Variation of Wear depth with Sliding Velocity (for Linear Element)

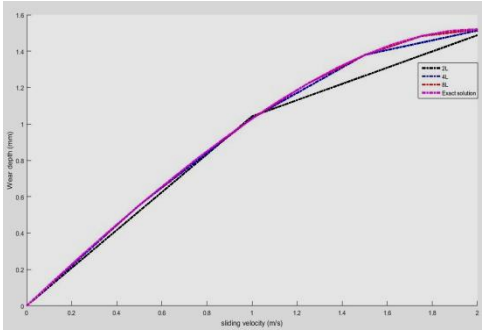

Fig 2: A graph of wear depth against change in Sliding Velocity

Variation of Wear depth with Contact Force

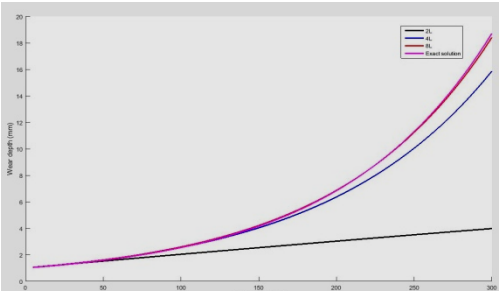

Force (N)

Fig 3: A graph of wear depth against change in force

5.0 Conclusion

Wear analysis of hot forging die has been solved with Galerkin's finite element method. The comparison of this study with exact solution shows a strong positive correlation which is an indication that this analysis is of higher accuracy and efficiency to predict abrasive wear in hot forging dies.

6.0 References

[1] Painter, B. Shivpuri, R. and Altan, T. (1996) "Prediction of Die wear during hot extrusion of engine valves". Journal of material processing technology, Vol. 59, pp.132-143.

[2] Huber, N., Okraft, O. Hegadekatte, V. (2006) "Modeling and Sinulation of Wear in a pin on disc tribometer" tribology letters, Volume 24, No.1, 59-60.

[3] Zamani, M. and Biglari, F. (2005) "Finite element investigation of wear in hot forging". Tehran International Congress on Manufacturing; Engineering, pp.1-9.

[4] Lejla Lavtar, Tadejmuchic, Goran Kugler, Milan Tercelj (2011) "Analysis of the main types of damage on a repair of industrial dies for hot forging car steering mechanisms". ELSEVIER, Engineering failure analysis 18, pp.1143-1152.

[5] Jhavar, S. Paul, C.P. and Javin, N.K. (2013) "Causes of failure and repairing options, for dies and molds", ELSEVIER, Engineering failure analysis. 34, pp519-535.

[6] Rachopol lamtanomchai and Sasithon Bland (2015) "study of wear and life enhancement of hot forging dies using finite element analysis. Proceeding of the world congress on engineering 2015, vol. 11 WCE 2015, July 1-3, 2015, London, U.K.

[7] Oviawe, C.I. (2017) "Development of a mathematical model for predicting abrasive wear in hot forging dies" Thesis submitted to the department of production engineering, University of Benin, Benin City. In partial fulfillment of the requirements for the award of doctor of philosophy (PhD) in manufacturing engineering in production engineering.

[8] Reddy, J.N. (1993). An introduction to the finite element method second edition McGraw-Hill, Inc.